CHAOS, CNN, MEMRISTORS AND BEYOND

The book is a unique collection of tributes to outstanding pioneer discoveries made by Leon Chua in nonlinear circuits, cellular neural networks, and chaos. The book is comprised of three parts. The first part — cellular nonlinear networks, nonlinear circuits and cellular automata — deals with Chua's Lagrangian circuits, cellular wave computers, bio-inspired robotics and neuro-morphic architectures, toroidal chaos, synaptic cellular automata, history of Chua's circuits, cardiac arrhythmias, local activity principle, symmetry breaking and complexity, bifurcation trees, and Chua's views on nonlinear dynamics of cellular automata. Dynamical systems and chaos is a scope of the second part of the book. There we find genius accounts on theory and application of Julia set, stability of dynamical networks, Chua's time, chaotic neural networks and neocortical dynamics, dynamics of piecewise linear systems, chaotic mathematical circuitry, synchronization of oscillators, models of catastrophic events, control of chaotic systems, symbolic dynamics, and solitons. First hand accounts on discovery of memristor in HP Labs, historical excursions into 'ancient memristors', analytical analysis of memristors, and hardware memristor emulators are presented in third part of the book.

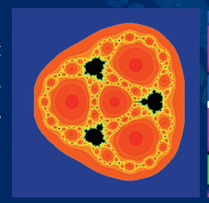

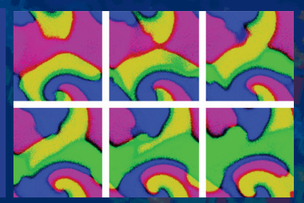

CHAOS, CNN, MEMRISTORS AND BEYOND

Adamatzky
Chen

CHAOS, CNN, MEMRISTORS AND BEYOND

Editors

Andrew Adamatzky
Guanrong Chen

World Scientific
www.worldscientific.com
8590 hc

ISBN 978-981-4434-79-9

World Scientific

CHAOS, CNN, MEMRISTORS AND BEYOND

A Festschrift for Leon Chua

Editors

Andrew Adamatzky
University of the West of England, UK

Guanrong Chen
City University of Hong Kong, P R China

World Scientific

NEW JERSEY · LONDON · SINGAPORE · BEIJING · SHANGHAI · HONG KONG · TAIPEI · CHENNAI

PREFACE

This edited compendium is dedicated to Professor Leon O. Chua on the occasion of his 75th birthday this year.

Given the advanced evolution and extreme specialization in science and technology today, a scientist may take great pride in the body of his work if, during his career, he has had a significant impact upon just a single area of science or engineering. But the impact of Professor Chua's work is in not just one, but no less than three areas: nonlinear circuit theory [1], cellular neural networks [2] and solid-state memristors [3].

The significance and impact of Leon's scientific work are evidenced by the large number of awards and honors he has received over his career, the most important of which include the conferring of 13 *Doctor Honoris Causa* (Honorary Doctorate) degrees from the following prestigious institutions:

- École Polytechnique Fédérale de Lausanne, Switzerland (1983)
- University of Tokushima, Japan (1984)
- Technische Universität Dresden, Germany (1992)
- Technical University of Budapest, Hungary (1994)
- University of Santiago de Compostela, Spain (1995)
- University of Frankfurt, Germany (1996)
- Gheorghe Asachi Technical University of Iaşi, Romania (1997)
- University of Catania, Italy (2000)
- AGH University of Science and Technology, Cracow, Poland (2003)
- Dogus University, Istanbul Turkey (2005)
- Université du Sud, Toulon, France (2006)
- Université du Havre, France (2009)
- University of the West of England, UK (2011).

In addition, Leon has received numerous prestigious awards and prizes for his work, including

- The IEEE Browder J. Thompson Memorial Prize Award (1967),
- The IEEE Guillemin-Cauer Award (1972, 1985, 1989),
- The IEEE W. R. G. Baker Prize Paper Award (1973),
- The Frederick Emmons Award (1974),
- The Alexander von Humboldt Senior US Scientist Award (1982),
- The IEEE Centennial Medal (1985),
- The IEEE Neural Networks Pioneer Award (2000),
- The IEEE Third Millenium Medal (2000),
- The IEEE Circuits and Systems Society Golden Jubilee Medal (2000),
- The IEEE Gustav Robert Kirchhoff Award (2005),
- The Mac E. Van Valkenburg Award (1995 and 1998),
- The IEEE Circuits and Systems Society Vitold Belevitch Award (2007),

- The Guggenheim Fellowship (2010),
- Leverhulme Visiting Professor, UK (2010–2011).

Most recently, Leon was appointed Distinguished Affiliated Professor by the Technische Universitat Muenchen (TUM), Germany, which is the highest honor of its kind, along with a lifelong academic appointment based in the TUM Department of Electrical Engineering and Information Technology. This particular honor is awarded "only to those exceptional scientists and researchers of international prominence that have significantly shaped their own disciplines and also inspired other areas within the scientific community." Other honorees of this award include Nobel Laureates such as Professor Rudolph A. Marcus (Chemistry).

Regarding Leon's education and career background, he received his BSEE degree from the Mapúa Institute of Technology in the Philippines in 1959, the MSEE from the Massachusetts Institute of Technology in 1961, and the Ph.D. from the University of Illinois at Urbana-Champaign in 1964. He then started to work as Assistant Professor of Electrical Engineering at Purdue University and was promoted to Associate Professor there in 1967. Finally, he joined the University of California at Berkeley in 1970 and taught there until he retired recently.

Leon is an IEEE Life Fellow (1974) and a foreign member of the European Academy of Sciences (1997) as well as of the Hungarian Academy of Sciences (2006). He owns seven USA patents, and is the recipient of the top 15 most-cited authors in 2002 from all fields of engineering published during the ten-year period (1991–2001) according to the ISI Current Contents database. He is also the Founding Editor-in-Chief of the *International Journal of Bifurcation and Chaos*.

Regarding his personal background, Leon Ong Chua (Chinese name 蔡少棠) was born on 28 June 1936. He and his family moved to the United States in 1959. Leon and his wife Diana have four daughters — Amy, Michelle, Katrin and Cynthia — and 7 grandchildren.

To commemorate Leon's 75th birthday, this volume is a collection of essays and research articles celebrating Leon's great achievements in science and technology written by some of his closest collaborators, former students and long-term friends; these articles present scientific works in areas related to nonlinear circuits, cellular neural networks, and memristors.

We wish to express our sincerest appreciation to the staff of World Scientific Publishing Company for their assistance in producing this book. We especially thank World Scientific's Chairman and Editor-in-Chief, Dr. K. K. Phua for his strong and enthusiastic support of this work honoring the achievements of Professor Leon O. Chua.

Andrew Adamatzky (University of Western England, UK)

Guanrong Chen (City University of Hong Kong, Hong Kong)

Co-Editors

Winter, 2011

References

[1] Matsumoto, T. [1984] "A chaotic attractor from Chua's circuit," *IEEE Trans. Circuits Syst.* **CAS-31**(12) 1055–1058.

[2] Chua, L. O. [1988] "Cellular neural networks: Theory," *IEEE Trans. Circuits Syst.* **CAS-35**(10) 1257–1272.

[3] Chua, L. O. [1971] "Memristor — the missing circuit element," *IEEE Trans. Circuits Th.* **18**(5) 507–519.

CONTENTS

CHAOS, CNN, MEMRISTORS AND BEYOND

A Festschrift for Leon Chua

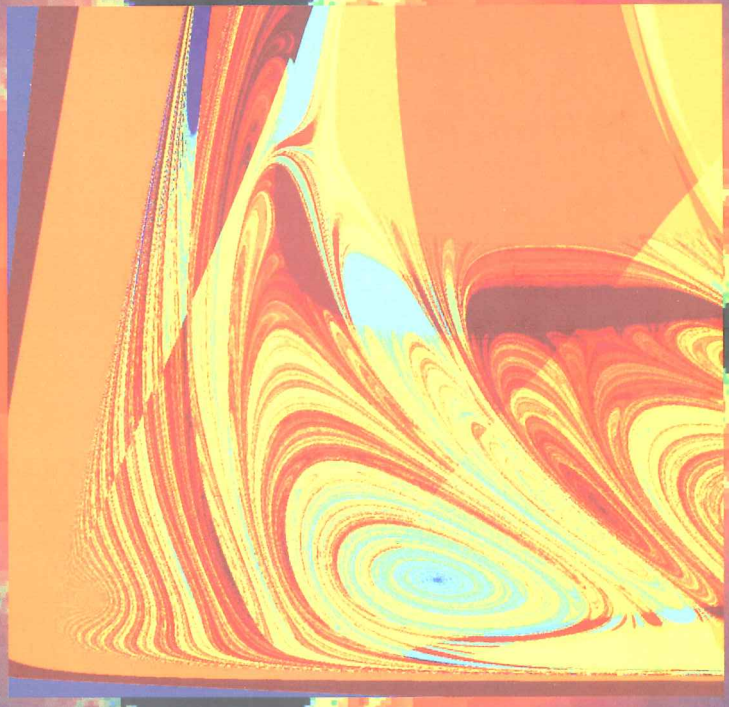

Editors

Andrew Adamatzky
Guanrong Chen

World Scientific

CHAPTER 33

SYMBOLIC DYNAMICS AND SPIRAL STRUCTURES DUE TO THE SADDLE-FOCUS BIFURCATIONS

ANDREY SHILNIKOV

Neuroscience Institute and Department of Mathematics and Statistics,
Georgia State University, Atlanta 30303, USA
ashilnikov@gsu.edu

LEONID SHILNIKOV
(17/12/1934–26/12/2011)

Institute for Applied Mathematics and Cybernetics,
Nizhniy Novgorod, 603006 Russia
diffequ@unn.ac.ru

ROBERTO BARRIO

Departamento de Matemática Aplicada and IUMA,
University of Zaragoza, E-50009. Spain
rbarrio@unizar.es

We examine spiral structures in bi-parametric diagrams of dissipative systems with strange attractors. We show that the organizing center for spiral structures in the Rössler model with the saddle-focus equilibria is related to the change of the structure of the attractor transitioning between the spiral and screw-like types. The structure skeleton is formed by saddle-node bifurcation curves originating from a codimension-two Belyakov point corresponding to the transition to the saddle-focus from a simple saddle. A new computational technique based on the symbolic kneading invariant description for examining dynamical chaos and parametric chaos in systems with Lorenz-like attractors is proposed and tested. This technique uncovers the stunning complexity and universality of spiral structures in the iconic Lorenz equations.

1. Introduction

Over recent years, a great deal of experimental studies and modeling simulations have been directed toward the identification of various dynamical and structural invariants to serve as key signatures uniting often diverse nonlinear systems into a single class.

One such class of low order dissipative systems has been identified to possess one common, easily recognizable pattern involving spiral structures in a biparametric phase space [2, 12, 13, 15]. Such patterns turn out to be ubiquitously alike in both time-discrete [30] and time-continuous systems [6, 20, 21].

Despite the overwhelming number of studies reporting the occurrence of spiral structures, there is still little known about the fine construction details and underlying bifurcation scenarios for these patterns. In this paper we study the genesis of the spiral structures in several low order systems and reveal the generality of underlying global bifurcations. We will start with the Rössler model and demonstrate that such parametric patterns are the key feature of systems with homoclinic connections involving saddle-foci meeting a single Shilnikov condition [44, 45]. The occurrence of this bifurcation causing complex dynamics is common for a plethora of dissipative systems, describing (electro)chemical reactions [32], population dynamics [26, 28], electronic circuits [12,19,40], including the Chua circuit [17,18]. The other group is made of models with the Lorenz attractor. Here, under consideration is the iconic Lorenz equation.

2. Spiral Hubs in Rössler-like Models

One of the most paradigmatic examples of low-dimensional deterministic chaos is the canonical Rössler system [33]:

$$\dot{x} = -(y + z), \quad \dot{y} = x + ay,$$
$$\dot{z} = b + z(x - c),$$

with two bifurcation parameters a and c (we fix $b = 0.2$). For $c^2 > 4ab$ the model has two equilibrium states, $P_{1,2}(ap_\pm, -p_\pm, p_\pm)$, where $p_\pm = (c \pm \sqrt{c^2 - 4ab})/2a$. This classical model exhibits the spiral and screw chaotic attractors after a period doubling cascade followed by the Shilnikov bifurcations of the saddle-focus P_2.

Bi-parametric screening of the Rössler model unveils a stunning universality of the periodicity

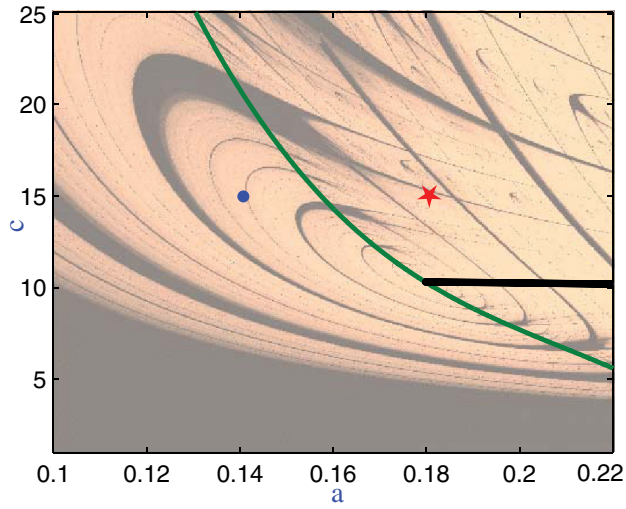

Fig. 1. Spiral structures in the biparametric bifurcation diagram of the Rössler model: light colors are associated with chaotic behavior, whereas dark colors correspond to regular, simple dynamics. The thick dark curve corresponds to the saddle-focus homoclinic bifurcation, and the medium green boundary separates the existence regions of the spiral (at •) and screw-shaped (at ⋆) attractors. Courtesy of [8].

hubs in the bifurcation diagrams shown in Fig. 1 [8]. The diagram is built on a dense grid of 1000×1000 points in the $(a\,c)$-parameter plane. Solutions of the model were integrated using the high precision ODE solver TIDES [1]. The color is related with the Lyapunov exponents, where dark and light colors discriminate between the regions of regular and chaotic dynamics corresponding to a zero and positive maximal Lyapunov exponent λ_1, respectively. The figure reveals the characteristic spiral patterns due to variations of the Lyapunov exponents.

The chaotic-regular regions spiral around a F[ocal] point [12, 13] at $(a, c) = (0.1798, 10.3084)$. This F-point terminates the bifurcation curve (black) corresponding to the formation of a homoclinic loop of the saddle-focus, P_2, in the phase space of the Rössler model [10]. Another curve (medium green) passes through the F-point: crossing it rightward the chaotic attractor in the phase space of the model changes the topological structure from spiral to screw-shaped. This curve has been identified from the examination of 1D Poincaré return maps (see Fig. 2) evaluated on a grid of 1000×1000 points.

The *spiral attractor* in the Rössler model at $a = 0.14$ (the point labeled by "•" in Fig. 1) generates a 1D unimodal map shown in the left panel of Fig. 2. In the case of the *screw attractor* at $a = 0.18$ (the point labeled by "⋆" in the diagram), the corresponding map shown in the right panel in Fig. 2 has

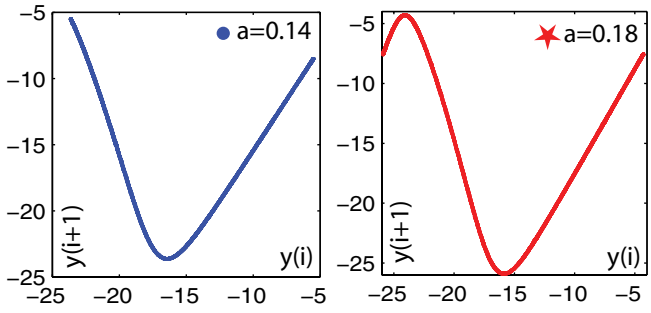

Fig. 2. 1D Poincaré return maps for the spiral and screw-shaped (resp.) chaotic attractors in the Rössler model at $a = 0.14$ and 0.18 for $c = 15$. Courtesy of [8].

a bimodal graph with two critical points. The addition of the second critical point in the map is indicative of a change of the topology of the attractors. This criteria was used to locate the corresponding boundary (medium green line) that separates the existence regions of the attractors of both types in the bifurcation diagram in Fig. 1 [8]. This boundary passes right through the F-point.

The dark bifurcation curve in Fig. 1 corresponds to a formation of the homoclinic orbits to the saddle-focus, P_2, of topological type (1,2), i.e. with 1D stable and 2D unstable manifolds, in the Rössler model. Depending on the magnitudes of the characteristic exponents of the saddle-focus, the homoclinic bifurcation can give rise to the onset of either rich complex or trivial dynamics in the system [22,44,45]. The cases under consideration meet the Shilnikov conditions and hence the existence of a single homoclinic orbit implies chaotic dynamics in the models within the parameter range in the presented diagrams. The magnification of the corresponding bifurcation curve in the diagram (Fig. 1) reveals that what appears to be a single bifurcation curve has actually two branches (Fig. 3). This curve has a U-shape with the turn at the F-point. Figure 3 shows the evolution of the homoclinic loops of the saddle-focus toward a simple saddle along the bifurcation curve. While its low branch corresponds to a primary loop, the upper branch corresponds to the double-pulse homoclinic loops. This suggests that the F-point actually might correspond to a heteroclinic cycle involving two equilibria, i.e. it is similar to T-points considered in the next section (actual study of the phase portrait for the parameter values corresponding to the F-point is yet to be done for the Rösler model).

Figure 4 outlines the structure of the bifurcation unfolding around the spiral hub [6, 8]. The picture depicts a number of the identified folded and cusp-shaped saddle-node bifurcation curves of periodic orbits originating from a codimension-two point, labeled as B[elyakov], toward the spiral hub in the (a, c)-parameter plane for the Rössler model. Note that none of these curves is actually a spiral — the overall spiral structure must be supported by homoclinic bifurcations. At this B-point, the saddle with real characteristic exponents becomes a saddle-focus for smaller values of the parameter a. The unfolding of this bifurcation is known [11] to contain bundles of countably many curves

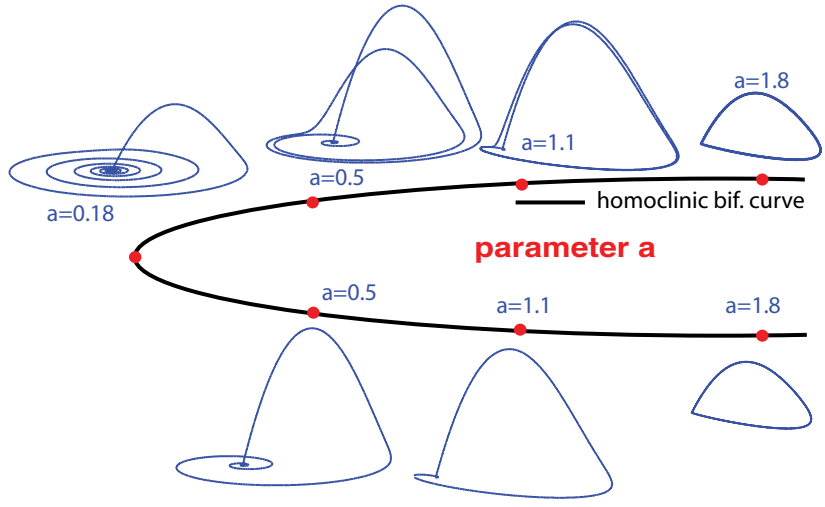

Fig. 3. Transformations of homoclinic orbits of the saddle-focus, P_2, in the Rössler system. In the sketch, the F-point is the turn point for two branches of the U-shaped bifurcation curve corresponding to the primary and secondary (with an additional round) homoclinic loops, which are sampled at the indicated points. Courtesy of [8].

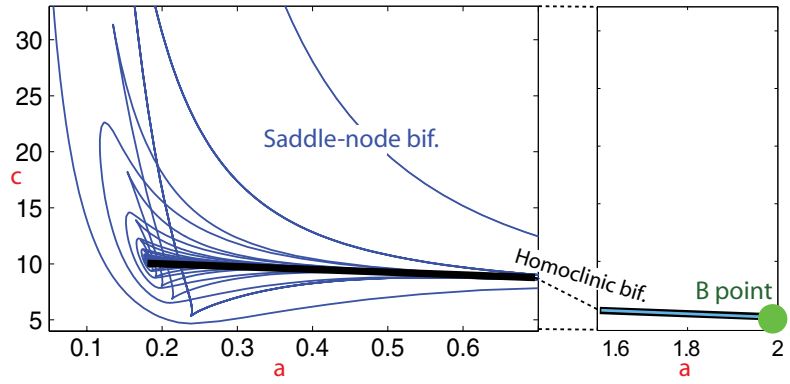

Fig. 4. Spiral structure is outlined with folded and cusp-shaped curves corresponding to saddle-node bifurcation of periodic orbits and originating from the codimension-two homoclinic B[elyakov]-point. Courtesy of [8].

corresponding to saddle-node and period doubling bifurcations of periodic orbits, as well as to various secondary homoclinic bifurcations of the saddle-focus. Indeed, both B- and F-points together globally determine the structure of the (a, c)-bifurcation portrait of the Rössler model [8].

3. Spiral Structures in Systems with the Lorenz Attractor

Dynamical systems theory is aimed to create purely abstract approaches followed by a further development of applicable tools allowing for the search and identification of basic invariants employed to unify diverse nonlinear systems with complex dynamics into a class. One such computationally justified approach for studying complex dynamics capitalizes on the concept of sensitivity of deterministic chaos. Sensitivity of chaotic trajectories can be quantified in terms of the divergence rate expressed through the largest Lyapunov characteristic exponent. The approach has been proven to work out exceptionally well for most systems with chaotic dynamics, like the Rössler model above. However, it has failed, in general, to deliver the desired answers and insights into intrinsic bifurcations of strange attractors in Lorenz-like models.

A strange attractor in the Lorenz equation from hydrodynamics has become a de-facto proof of deterministic chaos and the butterfly-shaped image of the iconic Lorenz attractor, shown in Fig. 5, has become the trademark of Chaos theory and dynamical systems. This theory elaborates on complex trajectory behaviors in nonlinear systems from mathematics, physics, life sciences, finance, etc. Universality of the methods along with bifurcation tools has made them spread wide and deep across all other disciplines.

3.1. *The Lorenz equation*

The Lorenz equation [29] is a system of three differential equations:

$$\dot{x} = -\sigma(x - y), \quad \dot{y} = r\,x - y - xz,$$
$$\dot{z} = -\frac{8}{3}z + xy, \tag{1}$$

with two positive bifurcation parameters: σ being the Prandtl number quantifying the viscosity of the fluid, and r being a Reynolds number used to characterize the fluid dynamics. Equation (1) is Z_2-symmetric: $(x, y, z) \leftrightarrow (-x, -y, z)$ [47].

Figure 6 (courtesy of [39]) exhibits the primary bifurcation curves (left panel) in the parameter plane, and depicts en route fragments of the formation of the Lorenz attractor on the pathway, $\sigma = 10$ [2, 27]. For $r < 1$, Eq. (1) has a single stable equilibrium state at the origin. This equilibrium state undergoes a pitch-fork bifurcation at $r = 1$, so that for $r > 1$ the origin becomes a saddle, O, of the topological type (2,1). This implies that the characteristic exponents of the linearized equation at O can be ordered as follows: $\lambda_3 < \lambda_2 < 0 < \lambda_1$. This implies also that the saddle has a pair of 1D separatrices (due to λ_1) leaving the saddle as $t \to +\infty$, and a 2D stable manifold containing the leading (due to λ_2) invariant z-axis. After the pitch-fork bifurcation, the outgoing separatrices of the saddle tend to two symmetric attractors — equilibrium states, $O_{1,2}(x = y = \pm\sqrt{\frac{8}{3}(r-1)}, z = r - 1)$ (Fig. 6(a)).

A homoclinic butterfly bifurcation occurs in the Lorenz equation when both 1D unstable

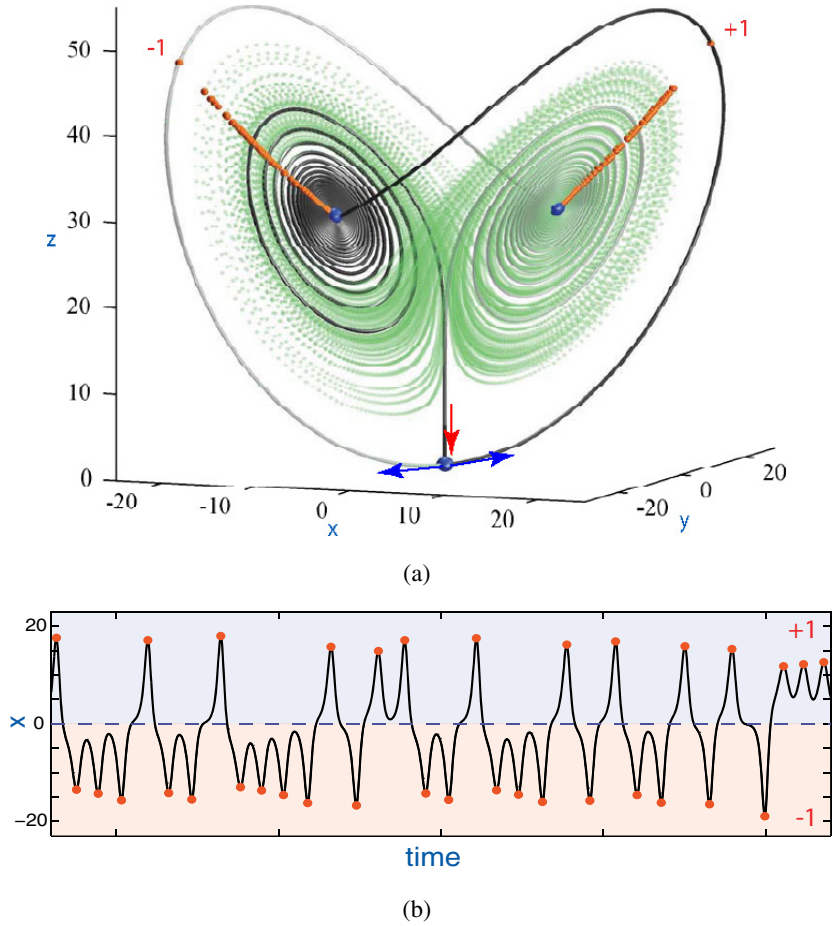

Fig. 5. (a) Heteroclinic connection (in dark color) between three saddles (blue spheres) overlaid with the Lorenz attractor (green light color) on the background in the 3D phase space of the Lorenz equation at the primary T-point ($r = 30.38$, $\sigma = 10.2$). Orange spheres on the butterfly wings indicating the turning points around the saddle-foci define the kneading sequence entries, $\{\pm 1\}$. (b) Time evolution of the x-coordinate of the right separatrix at other parameter values.

separatrices of the saddle come back to it along the z-axis (Fig. 6(b)). Bifurcations of the separatrices of the saddle at the origin are crucial overall for the Lorenz attractor. In virtue of the symmetry of the Lorenz equation, homoclinic loops come in pairs, and therefore constitute bifurcations of codimension-one, in general. The homoclinic butterfly bifurcation can be continued in the form of a continuous curve, l_1, in the (r, σ)-parameter plane of the Lorenz equation.

The very first homoclinic butterfly made of two separatrices looping a single round about the equilibrium states $O_{1,2}$, causes a homoclinic explosion in the phase space of the Lorenz equation; namely, this bifurcation gives rise to an enumerable set of saddle periodic orbits that further form the skeleton of the Lorenz chaotic set (yet to become the attractor). For the explosion to happen, the so-called *saddle value* $S = \lambda_1 + \lambda_2$, which is the sum of the leading characteristic exponents of the saddle, must be positive at the origin. Otherwise, the unfolding of the homoclinic butterfly produces a single symmetric figure-8 periodic orbit in the aftermath of a gluing bifurcation through which two stable periodic orbits merge into one after flowing into the homoclinic butterfly. In the case of the Lorenz equation with $S > 0$ at the origin, such saddle orbits demarcate a threshold of the "interior" of the chaotic unstable set (Fig. 6(c)).

After the homoclinic butterfly bifurcation, between $r_1 < r < r_2$, the separatrices of the saddle switch targets: now the right/left separatrix tends the left/right focus $O_{2/1}$. For the unstable chaotic set to become the Lorenz attractor, it must become invariant, i.e. must not lose trajectories running away to the stable foci $O_{1,2}$. This happens on another bifurcation curve, l_2, in the parameter space (Fig. 6(c)). After $r \geq r_2$, the Lorenz attractor

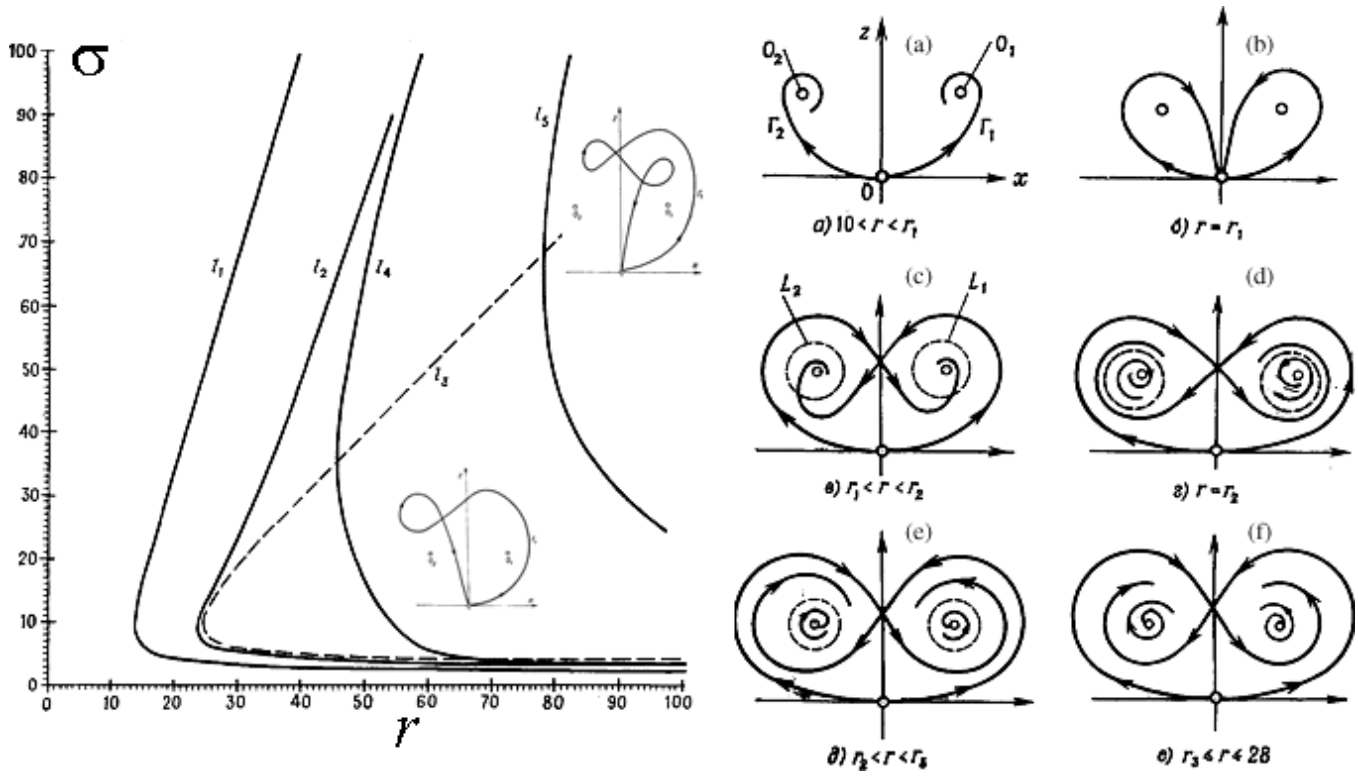

Fig. 6. (Left) The (r, σ)-parameter plane depicting the primary bifurcation curves and the stages of the formation of the Lorenz attractor. l_1 corresponds to the primary homoclinic butterfly; l_2 corresponds to the formation of the Lorenz attractor; l_3 is a supercritical Andronov-Hopf bifurcation curve; curves, l_4 and l_5, correspond to the homoclinic loops (in insets) with kneadings $\{+1, -1\}$ and $\{+1, -1, -1\}$, respectively. Courtesy of [39].

is shielded away from the stable equilibrium states by the 2D stable manifolds of the two "threshold" saddle orbits (Fig. 6(d)) that simultaneously emerge from each separatrix loop after crossing the curve l_1.

As r is increased to r_3 these periodic orbits collapse into the stable equilibria. The equilibrium states become saddle-foci of the (1,2)-type through a subcritical Andronov-Hopf bifurcation. The topological (1,2)-type means that each saddle-focus has 2D unstable and 1D stable manifolds; the latter is formed by two incoming separatrices. Some properties of the eigenvalues of the saddle-foci can be revealed without evaluating their characteristic exponents explicitly. Let $\lambda_1 < 0$ denote the stable exponent of $O_{1,2}$, and $\lambda_{2,3}$ stand for a complex conjugate pair such that $\mathrm{Re}\lambda_{2,3} > 0$. Observe that Eqs. (1) have a constant negative divergence given by $[-\sigma - 1 - 8/3]$, which equals $\sum_{i=1}^{3} \lambda_i$. This implies $\lambda_1 + \mathrm{Re}\lambda_{2,3} < 0$, i.e. the complex conjugate pair is closer to the imaginary axis than the real eigenvalue, and hence the saddle-foci meet the Shilnikov condition [43]. Therefore, if the saddle-focus has a homoclinic loop, the bifurcation causes the emergence of countably many periodic orbits near the saddle-focus. Those periodic orbits constantly undergo saddle-node and period doubling bifurcations as the parameters are varied. Moreover, since the Lorenz equation has the negative divergence, saddle-node bifurcations give rise to the onset of stable periodic orbits. Like in the case of the Rössler attractor, a single Shilnikov saddle-focus bifurcation can cause the emergence of spiral or screw-like attractors. However, a strange attractor due to the Shilnikov saddle-focus in a 3D system with a negative divergence is not a genuine chaotic one in the sense that it contains stable periodic orbits within, which may have large or narrow attraction basins in the phase space.

Because of that, such a chaotic attractor is called quasi-attractor thus referring to the existence of stable periodic orbits along with structurally unstable or non-transverse homoclinic orbits in the attractor [3, 40, 41]. Note that in higher dimension, one may have genuine strange attractors with a Shilnikov loop without stable periodic orbits (the so-called pseudo-hyperbolic attractors [40–42, 48]).

The Lorenz attractor is non-hyperbolic because it includes the origin — the saddle equilibrium

state of the topological type (2,1) while all other saddle periodic orbits are of the type (2,2), i.e. have 2D stable and unstable manifolds crossing transversally in the 3D phase space. In order for the Lorenz attractor to be strange and chaotic with no stable orbits, it may include neither [homoclinic] saddle-foci, $O_{1,2}$, nor contain only structurally stable homoclinic orbits due to transverse intersections of the manifolds of saddle periodic orbits.

After the stable equilibria are gone through the Andronov-Hopf bifurcation, the Lorenz equation exhibits the strange attractor of the iconic butterfly shape. The wings of the butterfly have symmetric eyes containing the saddle-foci are isolated from the trajectories of the Lorenz attractor. This attractor is structurally unstable [3,25] as it undergoes bifurcations constantly as the parameters of the equation are varied. The primary cause of structural and dynamical instability of chaos in the Lorenz equation and similar models is the singularity at the origin — the saddle with two one-dimensional outgoing separatrices. Both separatrices fill in densely two spatially symmetric, $[(x, y, z) \leftrightarrow (-x, -y, z)]$, wings of the Lorenz attractor in the 3D phase space (see Fig. 5). The Lorenz attractor undergoes a bifurcation when the separatrices of the saddle change the flip-flop pattern of switching between the butterfly wings centered around the saddle-foci. At the change, the separatrices comes back to the saddle thereby causing additional homoclinic explosions in the Lorenz attractor [2, 27].

The time progression of the "right" (or symmetrical "left") separatrix can be described geometrically and categorized in terms of the number of flip-flops around the equilibria $O_{1,2}$ in the 3D phase space of the Lorenz model (Fig. 5). An alternative way is to follow the time-evolution of the x-coordinate of the separatrix, which is shown in Panel B of Fig. 5. The sign-alternation of the x-coordinate suggests the introduction of a $\{\pm 1\}$-based alphabet to be employed for the symbolic description of the separatrix. Namely, whenever the right separatrix turns around O_1 or O_2, we write down $+1$ or -1, respectively. For example, the time series shown in Panel B generates the following kneading sequence starting with $\{+1, -1, -1, -1, +1, +1, +1, -1, \ldots\}$.

In what follows we demonstrate the new computational toolkit for the analysis of chaos in the Lorenz-like models. The toolkit is inspired by the idea of kneading invariants introduced by Milnor and Thurston [31]. A kneading invariant is a value that is intended to describe quantitatively the state of a complex system that admits a symbolic description using two symbols, here $+1$ and -1. The kneading invariant is supposed to depend monotonically on the parameter controlling the system so that any two systems can be compared and differentiated, or ordered in terms of $>$ and $<$, by the kneadings. Two systems with the same kneading are topologically conjugate [3, 25].

For the symmetric system with the Lorenz attractor, the kneading invariant is assigned to quantify the symbolic description of the separatrix. It reflects respectively and quantitatively a qualitative change in the separatrix behavior as the parameter of the system is changed. So, kneadings can serve as moduli of the topological equivalence to compare or contrast between any two Lorenz attractors or, equivalently, any two Lorenz-like systems.

In virtue of the spatial symmetry of the Lorenz equation, the kneading invariant for either separatrix is defined as a formal series:

$$P(q) = \sum_{n=0}^{\infty} \kappa_n \, q^n. \tag{2}$$

By setting $q \in (0, 1)$, the series (2) is made convergent. The sequence comprised with only $+1$ corresponds to the right separatrix (Fig. 5) tending to either an equilibrium state or a periodic orbit with $x(t) > 0$; the corresponding kneading invariant is given by $P_{\max} = 1/(1 - q)$. When the right separatrix converges to a ω-limit set with $x(t) < 0$ for all times; the corresponding kneading invariant is given $P_{min} = 1 - q/(1 - q)$ because the first $+1$ is followed by an infinite sequence of -1s. Thus, $[P_{\min}, P_{\max}]$ yields the range of the kneading invariant values.

In this computational study of the Lorenz equation we consider the very first 50 entries in the kneading sequences for the right separatrix of the saddle in order to generate the biparametric mapping: $(r, \sigma) \to P_{50}(q)$ with some appropriately chosen value of q. The mapping can be colorized using a non-linear spectrum ranging between to $P_{\min}^{(50)}$ and $P_{\max}^{(50)}$, respectively. In the mapping, a color is associated with a level curve corresponding to the particular value of the kneading invariant that remains constant for the given points in the parameter plane.

Figure 7 represents the kneading-based color mapping for the Lorenz equation in the parameter plane foliated by such kneading level curves on a dense grid of $[1000 \times 1000]$ points. In it, a wide window of a solid color corresponds to a constant

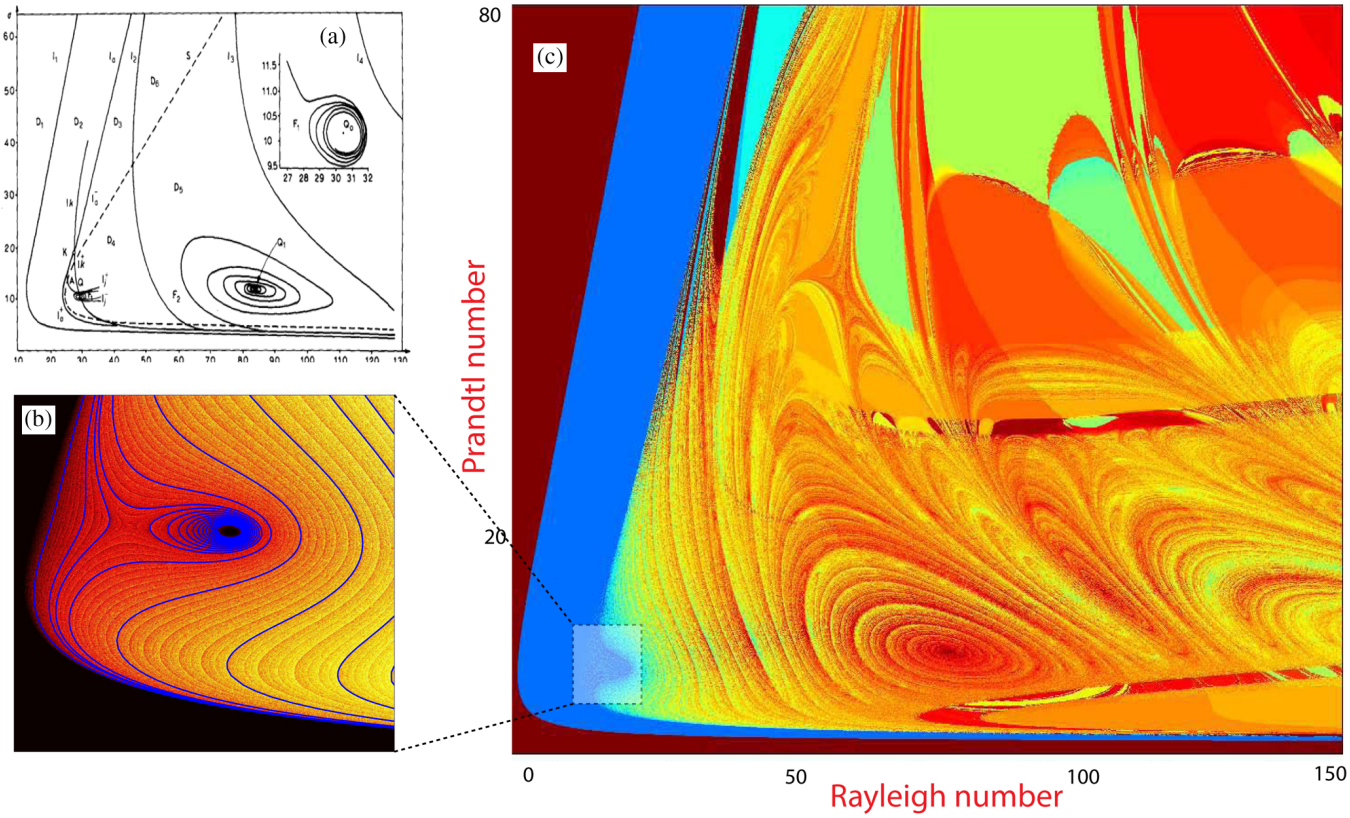

Fig. 7. (a) Bifurcation diagram of the Lorenz equation depicting the two detected T-points and primary homoclinic bifurcation curves (courtesy [15]). (c) The (r, σ)-biparametric sweeping revealing numerous T-points within a fractal mapping of the Lorenz equation in the kneading-based bifurcation diagram. Solid-color regions correspond to constant kneadings: dark (brown) region corresponding to simple Morse-Smale dynamics; lighter (blue) stripe corresponding to the chaotic saddle set after the homoclinic explosion due to the primary homoclinic butterfly. Bright (reddish) region maps the complex chaotic dynamics in the Lorenz equation globally organized by various T-points alternating with saddles in the parameter plane. (b) Zoom of the vicinity of the primary T-point at ($r = 30.4$, $\sigma = 10.2$) to which the homoclinic bifurcation curve converges. Data for curves (purple) are courtesy of Yu. Kuznetsov.

kneading. This implies that the behavior of the separatrix does not change within the windows. It could be due to the existence of robust trivial attractors such as equilibrium states or periodic orbits, to which the separatrix converges as time progress. The boundary between two solid-color regions corresponds to a bifurcation of the trivial attractor, which is associated with a jump between two constant values of the kneading invariant. For example, the jump from $P^{(50)}_{\max}$ to $P^{(50)}_{\min}$ in the kneading value occurs on the borderline between two regions, brown and light blue, corresponds to the formation of the homoclinic butterfly of the saddle. Since, for $r > 1$ there is a single Andronov-Hopf bifurcation for equilibria of the Lorenz equations, all other borderlines between the regions of solid colors should be associated with bifurcations of stable periodic orbits: period-doubling or saddle-nodes. A quick review of the kneading definition (2) suggests that the kneading value does not vary after a period-doubling bifurcation, because the kneading sequence will inherit the same coding; say original $[+1, -1, -1]$ will be repeated twice in the sequence $[+1, -1, -1, +1, -1, -1]$ for a new attractor of double period and so forth. The same is true also for the pitch-fork bifurcations, because continuous transitioning between stable symmetric and asymmetric periodic orbits is undetectable by the kneading technique. We can hypothesize that the borderlines may be only associated with generic saddle-node bifurcations, after which the separatrices must switch to another attractor with a distinct kneading invariant.

What the proposed kneading technique does extraordinary well, compared to the biparametric sweeping based on the finite-time maximal Lyapunov exponent approach, and what we have developed it for, is the detection of bifurcations of the

complex sets, see the parametric chaos in Fig. 7. Panel (b) of this figure depicts the kneading mapping at the left-bottom corner of the bifurcation diagram in panel (c). Here, the black (blue in Panel (c)) region corresponds to the unstable complex dynamics, while the region of the existence of the Lorenz attractor is presented in yellow-reddish colors. Dark (purple) curves singled out in panel (b) are bifurcation curves of the simplest homoclinic orbits with the shortest admissible kneadings. One can see from this panel that the diagram is nicely foliated by the kneading level curves of gradually progressing color from red to yellow. This indicates that the Lorenz attractor, while being structurally unstable and sensitive to parameter variations, persists the pseudo-hyperbolic property here because the foliation remains uniform, and transverse to the classical pathway $\sigma = 10$ (Fig. 6). This nice foliation starts breaking around a saddle point after which one partial bifurcation curve spirals onto a singular point. Far from this point, the curve corresponds to the formation of the homoclinic loop with the kneading $\{1, -1, -1, -1\}$, i.e. the right separatrix makes one excursion around the saddle-focus O_1, followed by three revolutions around the saddle-focus O_2, and then return to the saddle at the origin. While moving along the spiraling curve, the separatrix of the saddle makes progressively more turns around O_2. With each turn, the number of the scrolls around the spiral point increments progressively as well. Due to this feature the point $Q_1(r = 30.4, \sigma = 10.2)$ is called a Terminal or T-point, as the bifurcation curve spirals onto it so that the separatrix makes infinitely many turns. The limit case corresponds to the following symbolic sequence $\{+1, -1, -1, -1, \cdots\}$, or $\{+1, (-1)^{\infty}\}$. In virtue of the symmetry of the Lorenz equation, the T-point corresponds to a closed heteroclinic connection involving all three saddle-equilibria, see Fig. 5. The right (left) separatrix of the saddle merging with the incoming separatrix of the saddle-focus $O_2\,(O_1)$, makes the bifurcation increase the codimension to two, while intersections of the 2D unstable manifolds of the saddle-foci, with the 2D stable manifold of the saddle at the origin remain transverse. Breaking the 1D heteroclinic connection can give rise to a primary homoclinic orbit to the saddle-focus and to a heteroclinic connection between both saddle-foci. The corresponding bifurcation curves bound a sector originating from the T-point in the parameter plane as both r and σ are increased [15, 23]. Bykov [15] proved that near the primary T-point there are countably many alike T-points that are located within the sector. Each new T-point produces other non-overlapping sectors within self-similar structures scaled like fractals. Panel A shows two such identified T-points: primary and another secondary located at ($r = 85$, $\sigma = 11.9$). The primary codimension-two T-point in the Lorenz equation was originally discovered in [5].

As soon as the saddle-foci and their bifurcations become involved in the dynamics of the Lorenz attractor, it loses the purity of the genuine chaotic attractor that used to have neither stable periodic orbits nor non-transverse homoclinic trajectories, and transforms into a quasi-chaotic attractor with stable orbits and tangent homoclinics. The idea of non-transversality or tangency was employed in [14, 16] to numerically identify the second bifurcation curve, $l_{\rm K}$, in addition to the curve, l_2, that bounds the existence region of the Lorenz attractor in the parameter plane, see Fig. 8. Note that l_K crosses the initial boundary, l_2. This means that above the intersection point, crossing l_2 rightwards does not guarantee that the basin of the Lorenz attractor will necessarily be isolated from the stable foci, $O_{1,2}$ (Fig. 6). This means too that the

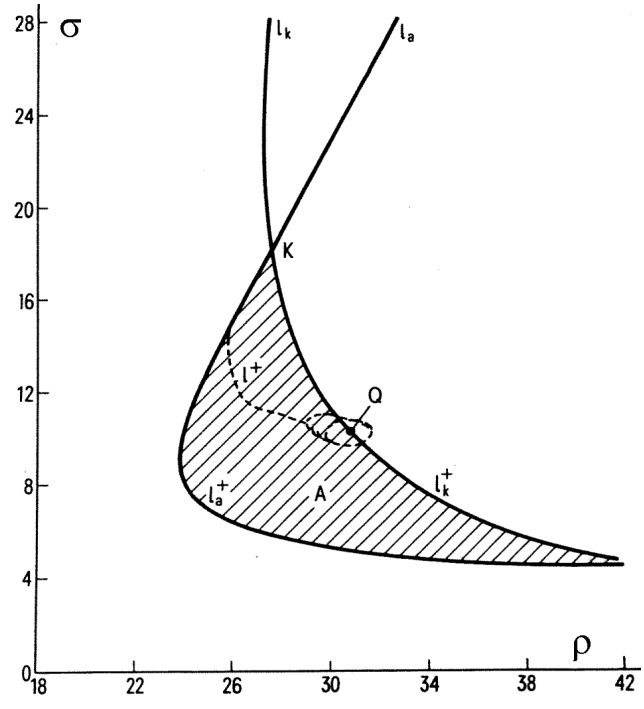

Fig. 8. The (r, σ)-bifurcation diagram showing the existence region (shaded) of the Lorenz attractor. The second bifurcation curve, l_k, passing through the primary T-point, $Q(r = 30.4,\ \sigma = 10.2)$, crosses the first boundary, l_a (l_2 in Fig. 6), thus closing the existence region. Courtesy of [16].

separatrices of the saddle will demonstrate some chaotic transient behaviors prior to them converging to $O_{1,2}$, see [16, 34–36, 38] for full details.

The other feature of the the boundary, l_K, is that it passes through the primary T-point, thereby separating the existence region of the Lorenz attractor from bifurcations of the saddle-foci, and consequently from all secondary T-points. So, for the parameter values to the right of the second boundary, the chaotic dynamics still persist in the Lorenz equation, and moreover it becomes more wider and less predictable [40–42, 48]. The indication to the saying is panel C of Fig. 7 showing chaos, turbulence in the parameter space, with fractal explosions in the forms of multiple spiral structures — "tornado eyes" centered around various T-points. Note that basins of spiraling T-points are separated by corresponding saddles in the parameter plane. One can spot self-similar smaller-scale spiral structures within large-scale ones and so forth. This richness of the structure of the parameter plane indicates that the chaotic attractor, which results from the synergy of the former Lorenz attractor amplified by chaos induced by the Shilnikov saddle-foci, becomes wild, in both dynamical and bifurcation senses.

Figure 9 shows a fragment of the typical biparametric sweeping of the Lorenz equation which is based on the evaluation of the largest Lyapunov exponent spectrum for the separatrices of the saddle calculated over a finite time interval. The same technique was used to identify the spiral structures in the Rössler model with the Shilnikov saddle-focus [6], and was employed in [24] for the study of a wild Lorenz attractor in the 3D Henon map, as well as to carry out a comprehensive three-parametric study of chaotic and regular regions of the Lorenz model [7,9,10]. In contrast to the Rössler model, the Lyapunov-exponent-based biparametric screening reveals no signs of indication of such structures within regions of deterministic chaos — including the Lorenz and quasi-attractors, where variations of the Lyapunov exponents are not significant enough to identify and differentiate between any fine patterns. These chaotic, red-colored regions in Fig. 9 are associated with positive values of the largest Lyapunov exponent, while the dark region corresponds to simple Morse-Smale dynamics with attractor having the largest Lyapunov exponent $L_{\max} \leq 0$ for stable equilibria or periodic orbits, respectively.

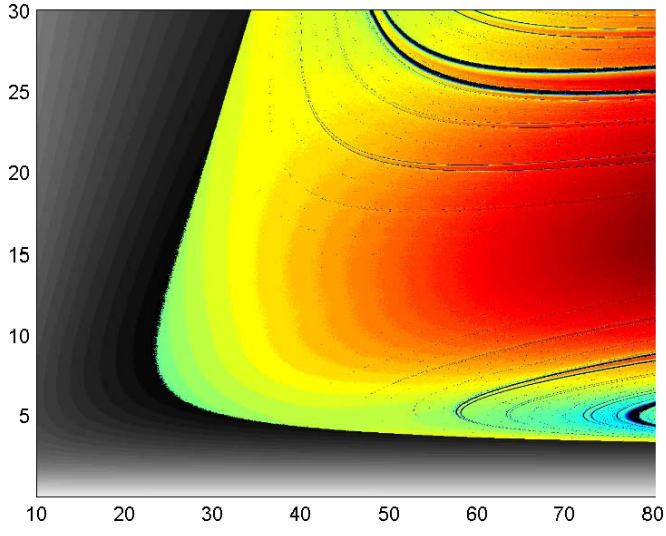

Fig. 9. Finite-time largest-Lyapunov exponent, $L_{\max}$, sweeping of the Lorenz equation shows no sign of spiral structures in the (r, σ)-parameter plane. The dark region corresponds to trivial attractors, where $L_{\max} \leq 0$, while the red color indicates the largest value of the maximal exponent, $L_{\max} > 0$, in chaotic regions right after the saddle-foci become involved.

4. Conclusions

We have examined two formation mechanisms of spiral structures in biparametric mappings of systems with the Shilnikov saddle-focus and with the Lorenz attractor. The feature of the spiral hubs in the Rössler model is that the F[ocal]-point gives rise to the alternation of the topological structure of the chaotic attractor transitioning between the spiral and screw-like types, as well as terminates the primary homoclinic curves of the saddle-focus equilibrium state influencing the forward-time dynamics of the model. The findings let us hypothesize about universality of the structure of the spiral hubs in similar systems with chaotic attractors due to homoclinics of the Shilnikov saddle-focus. The hub structures are outlined by homoclinic and saddle-node bifurcation curves originating from a codimension-two Belyakov point corresponding to the transition to the saddle-focus from a simple saddle.

For thorough explorations of the dynamics of Lorenz-like models we have proposed the algorithmically easy, though powerful toolkit based on the straight-forward evaluation of the kneading invariants derived through symbolic description of a single trajectory — an unstable separatrix of the saddle singularity of the model. We have demonstrated that the presence of multiple spiral T-points, saddles and

accompanying fractal structures in the parameter plane is the key signature for systems with the Lorenz attractor. The T-points partition and organize globally the bifurcation structures of the parameter space of a model with the Lorenz attractor. We point out that no other techniques, including approaches based on the Lyapunov exponents for example, can reveal the discovered parametric chaos with such stunning clarity and beauty.

The method should be beneficial for detailed studies of other systems admitting a reasonable symbolic description. It bears an education aspect: the kneading-based screening can be used for in-class presentation to reveal the magic and fascinating complexity of low-order models in the cross-disciplinary field of nonlinear dynamics. The bi-parametric mapping technique is easily adopted for parallel multicore GPU platforms allowing for ultra-fast simulations of models in questions. Additional implementation of high-precision computations for long transients will thoroughly reveal multi-layer complexity of self-similarity of fractal patterns of T-point vortices. In future research we intend to enhance the toolkits for exploration of high-dimensional systems, symmetric and asymmetric [37], admitting symbolic descriptions with more symbols and additional kneading invariants [49].

Acknowledgments

This work is supported by the Spanish Research projects MTM2009-10767 and MTM2012-31883 (to R.B.), and by NSF grant DMS-1009591, GSU Brain & Behaviors program, and MESRF "Attracting leading scientists to Russian universities" project 14.740.11.0919 (to A.S). We thank Dima Turaev for useful comments, Yu. Kuznetsov for sharing the data used in Fig. 7, Fernando Blesa and Sergio Serrano for sharing the data of Figs. 1, 2, 3 and 4, as well as Dane Allen, Bryce Chung and Joe Youker for careful proofreading the manuscript.

References

[1] Abad, A., Barrio, R., Blesa, F. and Rodríguez, M. (2013). Algorithm 924: TIDES, a Taylor series Integrator for Differential Equations, *ACM Transactions on Mathematical Software* **29**(1).

[2] Afraimovich, V., Bykov, V. V. and Shilnikov, L. P. (1977). The origin and structure of the Lorenz attractor, *Sov. Phys. Dokl.* **22**, pp. 253–255.

[3] Afraimovich, V., Bykov, V. V. and Shilnikov, L. P. (1983). On structurally unstable attracting limit sets of Lorenz attractor type, *Trans. Moscow Math. Soc.* **44**, 2, pp. 153–216.

[4] Afraimovich, V. and Shilnikov, L. (1983). Strange attractors and quasiattractors, in, *Dynamics and Turbulence, Pitman, NY*, pp. 1–51.

[5] Andreichikov, I. and Yudovich, V. (1972). Self-oscillating regimes branching from Poiseuille flow in a two-dimensional channel. *Dokl. Akad. Nauk SSSR* **17**, pp. 120–124.

[6] Barrio, R., Blesa, F. and Serrano, S. (2009). Qualitative analysis of the Rössler equations: bifurcations of limit cycles and chaotic attractors, *Phys. D* **238**, 13, pp. 1087–1100.

[7] Barrio, R., Blesa, F. and Serrano, S. (2012). Behavior patterns in multiparametric dynamical systems: Lorenz model, *Internat. J. Bifur. Chaos* **22**(6), p. 1230019 (14 pages).

[8] Barrio, R., Blesa, F., Serrano, S. and Shilnikov, A. (2011b). Global organization of spiral structures in bi-parameter space of dissipative systems with Shilnikov saddle-foci, *Phys. Rev. E* **84**, 035201.

[9] Barrio, R. and Serrano, S. (2007). A three-parametric study of the Lorenz model, *Phys. D* **229**, 1, pp. 43–51.

[10] Barrio, R. and Serrano, S. (2009). Bounds for the chaotic region in the Lorenz model, *Phys. D* **238**, 16, pp. 1615–1624.

[11] Belyakov, L. A. (1980). The bifurcation set in a system with a homoclinic saddle curve, *Mat. Zametki* **28**, 6, pp. 911–922, 962.

[12] Bonatto, C. and Gallas, J. A. C. (2008). Periodicity hub and nested spirals in the phase diagram of a simple resistive circuit, *Phys. Rev. Lett.* **101**, 5, p. 054101.

[13] Bonatto, C., Garreau, J. C. and Gallas, J. A. C. (2005). Self-similarities in the frequency-amplitude space of a loss-modulated CO_2 laser, *Phys. Rev. Lett.* **95**, 14, p. 143905.

[14] Bykov, V. and Shilnikov, A. (1989). Boundaries of the domain of existence of a Lorenz attractor, *Methods in qualitative theory and bifurcation theory (in Russian)* **1**, pp. 151–159.

[15] Bykov, V. V. (1993). The bifurcations of separatrix contours and chaos, *Phys. D* **62**, 1-4, pp. 290–299.

[16] Bykov, V. V. and Shilnikov, A. L. (1992). On the boundaries of the domain of existence of the Lorenz attractor, *Selecta Math. Soviet.* **11**, 4, pp. 375–382.

[17] Chua, L. (1994). Chuas circuit : An overview ten years later,, *J. Circuits, Systems and Computers* **4**, pp. 117–159.

[18] Chua, L. (2007). Chua circuit, *Scholarpedia* **2**(10), p. 1488.

[19] Freire, J. G. and Gallas, J. A. C. (2010). Non-shilnikov cascades of spikes and hubs in a

semiconductor laser with optoelectronic feedback, *Phys. Rev. E* **82**, 3, p. 037202.

[20] Gallas, J. A. C. (2010). The structure of infinite periodic and chaotic hub cascades in phase diagrams of simple autonomous flows, *Internat. J. Bifur. Chaos* **20**, 2, pp. 197–211.

[21] Gaspard, P., Kapral, R. and Nicolis, G. (1984). Bifurcation phenomena near homoclinic systems: A two-parameter analysis, *J. Statist. Phys.* **35**, pp. 697–727.

[22] Gaspard, P. and Nicolis, G. (1983). What can we learn from homoclinic orbits in chaotic dynamics? *J. Statist. Phys.* **31**, 3, pp. 499–518.

[23] Glendinning, P. and Sparrow, C. (1984). Local and global behavior near homoclinic orbits, *J. Statist. Phys.* **35**, 5–6, pp. 645–696.

[24] Gonchenko, S., Ovsyannikov, I., Simo, C. and Turaev, D. (2005). Three-dimensional Hénon-like maps and wild Lorenz-like attractors, *Internat. J. Bifur. Chaos* **15**(11), pp. 3493–3508.

[25] Guckenheimer, J. and Williams, R. F. (1979). Structural stability of Lorenz attractors, *Inst. Hautes Études Sci. Publ. Math.* **50**, 50, pp. 59–72.

[26] Hastings, A. and Powell, T. (1991). Chaos in a three-species food chain, *Ecol.* **72**, pp. 896–903.

[27] Kaplan, J. L. and Yorke, J. A. (1979). Preturbulence: a regime observed in a fluid flow model of Lorenz, *Comm. Math. Phys.* **67**, 2, pp. 93–108.

[28] Kuznetsov, Y. A., De Feo, O. and Rinaldi, S. (2001). Belyakov homoclinic bifurcations in a tritrophic food chain model, *SIAM J. Appl. Math.* **62**, 2, pp. 462–487.

[29] Lorenz, E. (1963). Deterministic nonperiodic flow, *J. Atmospheric Sci.* **20**, pp. 130–141.

[30] Lorenz, E. N. (2008). Compound windows of the Hénon-map, *Phys. D* **237**, 13, pp. 1689–1704.

[31] Milnor, J. and Thurston, W. (1988). On iterated maps of the interval, *Lecture Notes in Math.* **1342**, pp. 465–563.

[32] Nascimento, M. A., Gallas, J. A. C. and Varela, H. (2011). Self-organized distribution of periodicity and chaos in an electrochemical oscillator, *Phys. Chem. Chem. Phys.* **13**, pp. 441–446.

[33] Rössler, O. E. (1976). An equation for continuous chaos, *Phys. Lett. A* **57**, 5, pp. 397–398.

[34] Shilnikov, A. (1986). Bifurcations and chaos in the Marioka-Shimizu model. Part I. *Methods in qualitative theory and bifurcation theory (in Russian)* **1**, pp. 180–193.

[35] Shilnikov, A. (1989). Bifurcations and chaos in the Marioka-Shimizu model. Part II. *Methods in qualitative theory and bifurcation theory (in Russian)* **1**, pp. 130–198.

[36] Shilnikov, A. (1991). Bifurcation and chaos in the Morioka-Shimizu system, *Selecta Math. Soviet.* **10**(2), pp. 105–117.

[37] Shilnikov, A. and Shilnikov, L. (1991). On the nonsymmetric lorenz model, *Internat. J. Bifur. Chaos* **1**, pp. 773–776.

[38] Shilnikov, A. L., Shilnikov, L. P. and Turaev, D. V. (1993). Normal forms and Lorenz attractors, *Internat. J. Bifur. Chaos* **3**, 5, pp. 1123–1139.

[39] Shilnikov, L. (1980). Bifurcation theory and the Lorenz model. *Appendix to Russian edition of "The Hopf Bifurcation and Its Applications."* Eds. J. Marsden and M. McCraken., pp. 317–335.

[40] Shilnikov, L. (1994). Chua's circuit: Rigorous results and future problems, *Internat. J. Bifur. Chaos* **4**(3), pp. 489–518.

[41] Shilnikov, L. (1997). Mathematical problems of nonlinear dynamics: A tutorial. visions of nonlinear mechanics in the 21st century, *Journal of the Franklin Institute.* **334**(5–6), pp. 793–864.

[42] Shilnikov, L. (2002). Bifurcations and strange attractors, *Proc. Int. Congress of Mathematicians, Beijing (China) (Invited Lectures).* **3**, pp. 349–372.

[43] Shilnikov, L. and Shilnikov, A. (2007). Shilnikov bifurcation, *Scholarpedia* **2**(8), p. 1891.

[44] Shilnikov, L. P. (1965). A case of the existence of a countable number of periodic motions, *Sov. Math. Dokl.* **6**, p. 163.

[45] Shilnikov, L. P., Shilnikov, A. L., Turaev, D. and Chua, L. O. (2001). *Methods of qualitative theory in nonlinear dynamics. Part II* (World Scientific Publishing Co. Inc.).

[46] Shilnkov, A. (1993). On bifurcations of the Lorenz attractor in the Shimizu-Morioka model, *Physica D* **62**(1–4), pp. 338–346.

[47] Sparrow, C. (1982). *The Lorenz equations: bifurcations, chaos, and strange attractors*, Applied Mathematical Sciences, Vol. 41 (Springer-Verlag, New York).

[48] Turaev, D. and Shilnikov, L. (1998). An example of a wild strange attractor, *Sbornik. Math.* **189**(2), pp. 291–314.

[49] Barrio, R., Shilnikov, A. and Shilnikov, L. P. (2012). Kneadings, symbolic dynamics, and painting Lorenz chaos. A Tutorial, *Internat. J. Bifur. Chaos* **22**(4), 1230016.